HbtR, a heterofunctional homolog of the virulence regulator TcpP, facilitates the transition between symbiotic and planktonic lifestyles in *Vibrio fischeri*.

Brittany D. Bennett, Tara Essock-Burns, and Edward G. Ruby

Pacific Biosciences Research Center, University of Hawai‘i—Manoa, Honolulu, HI 96813

Running head: Regulation of lifestyle transition in *V. fischeri*

Address correspondence: eruby@hawaii.edu

Abstract

The bioluminescent bacterium *Vibrio fischeri* forms a mutually beneficial symbiosis with the Hawaiian bobtail squid, *Euprymna scolopes*, in which the bacteria, housed inside a specialized light organ, produce light used by the squid in its nocturnal activities. Upon hatching, *E. scolopes* juveniles acquire *V. fischeri* from the seawater through a complex process that requires, among other factors, chemotaxis by the bacteria along a gradient of *N*-acetylated sugars into the crypts of the light organ, the niche in which the bacteria reside. Once inside the light organ, *V. fischeri* transitions into a symbiotic, sessile state in which the quorum-signaling regulator LitR induces luminescence. In this work we show that expression of *litR* and luminescence are repressed by a homolog of the *V. cholerae* virulence factor TcpP, which we have named HbtR. Further, we demonstrate that LitR represses genes involved in motility and chemotaxis into the light organ and activates genes required for exopolysaccharide production.

Importance

TcpP homologs are widespread throughout the *Vibrio* genus; however, the only protein in this family described thus far is a *V. cholerae* virulence regulator. Here we show that HbtR, the TcpP homolog in *V. fischeri*, has both a biological role and regulatory pathway completely unlike that in *V. cholerae*. Through its repression of the quorum-signaling regulator LitR, HbtR affects the expression of genes important for colonization of the *E. scolopes* light organ. While LitR becomes activated within the crypts, and upregulates luminescence and exopolysaccharide genes and downregulates chemotaxis and motility genes, it appears that HbtR, upon expulsion of *V. fischeri* cells into seawater, reverses this process to aid the switch from a symbiotic to a planktonic state. The

40 possible importance of HbtR to the survival of *V. fischeri* outside of its animal host may
41 have broader implications for the ways in which bacteria transition between often vastly
42 different environmental niches.
43

44 **Introduction**

45 The Gram-negative bacterium *Vibrio (Aliivibrio) fischeri* is a model organism for the
46 study of biochemical processes underpinning bioluminescence, quorum sensing, and
47 bacterial-animal symbioses. Luminescence in *V. fischeri* is activated by a quorum-
48 sensing pathway that responds to high concentrations of two autoinducer molecules, *N*-
49 (3-oxohexanoyl)-L-homoserine lactone (3-oxo-C6-HSL (1)) and *N*-octanoyl-L-
50 homoserine lactone (C8-HSL (2)). When *V. fischeri* cells multiply to a certain density, 3-
51 oxo-C6-HSL and C8-HSL accumulate to high local concentrations, initiating a signaling
52 cascade that leads to upregulation of the regulator LuxR by the regulator LitR and
53 consequent activation of the luciferase operon, *luxICDABEG* (3–5); reviewed in (6).
54 Light production by *V. fischeri* is a crucial factor in the mutualistic symbiosis it
55 forms within the light-emitting organ of the Hawaiian bobtail squid, *Euprymna scolopes*
56 (7–9). Juvenile *E. scolopes* become colonized with *V. fischeri* shortly after hatching into
57 seawater containing this bacterium (10). *V. fischeri* cells initiate light-organ colonization
58 through a series of steps, including chemotaxis towards *N*-acetylated sugars released
59 by the squid (11, 12). After initial colonization of the squid light organ, the symbiosis
60 undergoes a daily cyclic rhythm of three basic stages for the remainder of the squid's
61 life: during the day, *V. fischeri* cells grow to a high density in the crypts on carbon
62 sources provided by the squid (13, 14); at night, the bacteria produce light that aids in

63 camouflage for the squid (15, 16); and at dawn, ~95% of the bacterial cells are expelled
64 from the light organ into the seawater, where they may initiate colonization of new squid
65 hatchlings, while the remaining ~5% repopulate the light organ (17, 18).

66 Previous work indicated that, in *V. fischeri* cells newly expelled from the light
67 organ, numerous genes are up- and downregulated relative to their level of expression
68 in cells that had been planktonic for some time (19). Two of the genes upregulated in
69 expelled cells were VF_A0473 and VF_A0474, comprising a small operon annotated as
70 encoding homologs of the genetic regulator TcpP and its chaperone, TcpH. TcpP was
71 first described in *V. cholerae* as a virulence gene regulator (20, 21). During the early
72 stages of *V. cholerae* infection, TcpP works synergistically with another transcriptional
73 regulator, ToxR, to upregulate expression of the virulence regulator *toxT* and thereby
74 activate expression of cholera toxin and the toxin-coregulated pilus in response to
75 changing environmental conditions (21, 22). *tcpPH* expression is itself induced by AphA
76 and AphB in response to low oxygen or acidic pH (23–25). In *V. cholerae* El Tor
77 biotypes, *aphA* expression is repressed by HapR (the *V. cholerae* ortholog of LitR) upon
78 initiation of quorum sensing at high cell densities (26, 27). Additionally, activation of
79 *tcpPH* expression by AphA and AphB is inhibited by the global metabolic regulator Crp
80 (28). This complex regulatory pathway serves to upregulate *tcpPH* and, consequently,
81 downstream virulence factors under conditions consistent with entry into the vertebrate
82 gut, a process reversed late in the infection cycle before the bacteria exit the host and
83 re-enter an aquatic environment (29, 30).

84 No published genomes of *V. fischeri* strains encode homologs of either *toxT* or
85 cholera toxin genes. The genome of the model strain *V. fischeri* ES114 does encode

86 annotated homologs of the toxin-coregulated pilus genes *tcpFETSD* and *tcpCQBA*, but
87 this strain is alone among the 66 currently available *V. fischeri* genomes to do so. The
88 *V. fischeri* genes regulated by the protein product of VF_A0473 are therefore unknown,
89 as are any upstream regulatory factors that determine under which conditions the
90 regulator is produced and active. Here we present evidence that VF_A0473 regulates
91 genes governing phenotypes relevant to the switch from symbiosis to a planktonic
92 lifestyle. We therefore rename VF_A0473 and VF_A0474, currently annotated as *tcpP*
93 and *tcpH*, as *hbtR* (*hab*itat *t*ransition *r*egulator) and *hbtC* (*hab*itat *t*ransition *c*haperone).
94 In this work, we identify the HbtR regulon and uncover aspects of *hbtRC* regulation.
95 Further, we determine that LitR is repressed by HbtR and describe LitR-regulated
96 phenotypes beyond luminescence that are important for light-organ colonization.
97

98 **Results**

99 <u>The HbtR regulon is distinct from that of TcpP.</u> Considering that *V. fischeri* and *V.*
100 *cholerae* have significantly different lifestyles, as well as the absence in 65 of 66
101 sequenced *V. fischeri* genomes of homologs of virulence-factor genes regulated by
102 TcpP in *V. cholerae*, we postulated that HbtR has a distinct function from that of TcpP.
103 To determine the regulon of HbtR, RNA-seq was performed using Δ*hbtRC* mutant
104 strains of *V. fischeri* ES114 carrying either empty vector or an inducible vector with
105 *hbtRC* under control of the *lac* promoter. Notable among the RNA-seq results (Table
106 S1) is that none of the *tcp* pilus gene homologs encoded in the *V. fischeri* ES114
107 genome were expressed at significantly different levels in *hbtRC* strains carrying either

108 empty vector or the inducible *hbtRC* vector (Table S1), ruling out the possibility that
109 HbtR regulates the same genes in *V. fischeri* ES114 as TcpP does in *V. cholerae*.
110
111 HbtR represses *litR* expression and luminescence *in vitro.* Among the genes
112 significantly downregulated in the RNA-seq results when *hbtRC* was expressed were
113 the quorum signaling-regulated genes *litR*, *luxR*, *qsrP*, and *rpoQ* (Table 1, Table S1).
114 Less strongly, but statistically significantly, downregulated genes included most of the
115 luciferase operon (Table 1, Table S1). To determine whether repression of *lux* genes by
116 HbtR affects bacterial light emission, luminescence and growth were monitored in
117 cultures of wild-type *V. fischeri* and its Δ*hbtRC* derivative carrying either empty vector or
118 vector constitutively expressing *hbtRC*. Deletion of *hbtRC* did not affect light production;
119 however, overexpression of *hbtRC* in either wild type or Δ*hbtRC* led to a delay in onset
120 and significant decrease in intensity of light production (Fig. 1A). There was no
121 difference in growth rate between the strains (Fig. 1B), eliminating the possibility that
122 the reduced luminescence by the *hbtRC*-overexpression strains was due to a growth
123 defect. To determine whether deletion of *hbtRC* would lead to a change in light
124 production by *V. fischeri* within the light organ, *E. scolopes* hatchlings were colonized
125 with wild-type *V. fischeri* or Δ*hbtRC*. There was no difference in the luminescence of
126 juvenile squid colonized by either *V. fischeri* strain at either 24 or 48 h (Fig. S1),
127 suggesting that HbtR is not active inside the light organ.
128
129 HbtR activates and LitR represses chemosensory genes involved in *E. scolopes* light-
130 organ colonization. Among the genes upregulated in the *hbtRC*-expressing strain in the

131 RNA-seq experiment were four genes annotated as encoding methyl-accepting
132 chemotaxis proteins (MCPs): VF_1133, VF_2042, VF_A0246, and VF_A0389 (Table 1,
133 Table S1). To confirm that the upregulation of these MCP genes by HbtR functions
134 through its repression of *litR* expression, RT-qPCR was performed on wild-type *V.*
135 *fischeri* and Δ*litR*, as well as Δ*hbtRC* carrying either empty vector or vector
136 constitutively expressing *hbtRC*. Expression of all four of these MCP genes was
137 significantly increased in Δ*litR* compared to wild-type *V. fischeri* (Table 2). Expression of
138 VF_2042 was significantly increased in Δ*hbtRC* constitutively expressing *hbtRC*
139 compared to Δ*hbtRC* carrying empty vector (Table 2), confirming the RNA-seq results
140 indicating that HbtR affects MCP gene regulation.

141 As chemotaxis is essential to colonization of the *E. scolopes* light organ by *V.*
142 *fischeri* (12), we asked whether any of the four MCPs repressed by LitR are involved in
143 colonization. Newly hatched *E. scolopes* juveniles were exposed to a 1:1 ratio of wild-
144 type *V. fischeri* and a quadruple mutant with in-frame deletions of all four of the LitR-
145 repressed MCP genes (ΔVF_1133ΔVF_2042ΔVF_A0246ΔVF_A0389; "ΔΔΔΔ").
146 Regardless of which strain carried a *gfp*-labeled plasmid, the squid light organ
147 populations tended to be dominated by wild-type *V. fischeri* (Fig. 2), indicating that HbtR
148 and LitR regulate chemotaxis genes involved in initiating symbiosis.

149 To determine whether the colonization defect displayed by ΔΔΔΔ is due to the
150 chemosensory function of any of the four MCP genes, we sought to identify the
151 chemoattractants recognized by these MCPs. Wild-type *V. fischeri* and MCP deletion
152 mutants were spotted onto minimal-medium, soft-agar plates containing 1 mM of three
153 known chemoattractants for *V. fischeri* (12): *N*-acetyl-D-glucosamine (GlcNAc), *N*,*N'*-

154 diacetylchitobiose ($(GlcNAc)_2$), or *N*-acetylneuraminic acid (Neu5Ac). The chemotactic
155 zone sizes for ΔVF_1133 and ΔVF_A0246 were significantly smaller than for wild-type
156 *V. fischeri* on each of the *N*-acetylated sugars (Table 3). Oddly, while the zone sizes of
157 ΔΔΔΔ on GlcNAc and $(GlcNAc)_2$ were similar to those of ΔVF_1133 and ΔVF_A0246,
158 on Neu5Ac the ΔΔΔΔ zone size was comparable to wild type. This is a repeatable
159 phenotype we have yet to explain. However, a ΔVF_1133 ΔVF_A0246 mutant produced
160 a similar zone size to the single mutants on Neu5Ac. There was no significant difference
161 in zone sizes between ΔΔΔΔ and wild-type *V. fischeri* spotted onto plates containing
162 either no chemoattractant or 1 mM glucose (Table 3), indicating these mutations do not
163 affect motility or chemotaxis in general. Because they grew equally well on either
164 GlcNAc or Neu5AC (Fig. S2), the differences in zone sizes of the MCP mutants and
165 wild-type *V. fischeri* were unlikely to be growth-related.
166
167 <u>HbtR activates and LitR represses motility.</u> Two flagellin genes, *flaC* and *flaF*, were
168 upregulated by *hbtRC* (Table 1, Table S1), indicating the possible activation of motility
169 by HbtR. An earlier study demonstrated that LitR represses motility in *V. fischeri* (31),
170 and microarrays performed previously (Studer, Schaefer, and Ruby; Schaefer and Ruby
171 unpublished data) indicated that AinS and LitR downregulate the expression of a
172 majority of the flagellin genes within the locus VF_1836–77, as well as *flaF*, *fliL2*, *motX*,
173 *motA1B1*, and *cheW*. To confirm the repression of motility genes by LitR, RT-qPCR was
174 employed to determine the level of expression of three flagellin or motor genes in
175 different genomic regions in wild-type *V. fischeri* and Δ*litR*. Expression of *cheW*, *motA1*,
176 *flaC*, and *flaF* was moderately, but statistically significantly, higher in Δ*litR* than in wild-

177 type *V. fischeri* (Table 2). However, we were not able to determine the mechanism by
178 which LitR represses multiple motility gene loci, as expression levels of the known
179 flagellin regulatory genes *rpoN*, *flrA*, *flrB*, *fliA*, and *flgM* were comparable between Δ*litR*
180 and wild-type *V. fischeri* strains (Table 2).

181 The sigma factor-like regulator RpoQ, which is upregulated by LitR, represses
182 motility and/or chemotaxis towards GlcNAc when overexpressed (32). Thus, we wanted
183 to determine whether the effect LitR has on motility and *N*-acetylated sugar chemotaxis
184 is mediated through its regulation of *rpoQ*. On soft-agar chemotaxis plates containing no
185 chemoattractant or 1 mM GlcNAc, we observed the same pattern regardless of the
186 presence of GlcNAc: either deletion of *litR* or overexpression of *hbtRC* led to larger
187 migration zones than for wild-type *V. fischeri*, while overexpression of *litR* essentially
188 eliminated bacterial migration (Table 3). There were no significant differences between
189 Δ*rpoQ* and wild-type *V. fischeri* strains carrying the same vector (Table 3), indicating
190 that the repression of motility by LitR is not mediated through RpoQ.

191

192 <u>HbtR represses and LitR activates exopolysaccharide production</u>. An approximately 25-
193 kb locus constituting the genes VF_0157–80 was downregulated when *hbtRC* was
194 expressed (Table 1, Table S1). Previously performed microarrays indicated that most of
195 the genes in this locus (VF_0159 and VF_0162–0180) are also upregulated by AinS
196 and LitR (Studer, Schaefer, and Ruby; Schaefer and Ruby, unpublished data). To
197 confirm the upregulation of this locus by LitR, RT-qPCR was used to evaluate the
198 expression of three genes, located in separate operons, in Δ*litR* and wild-type *V.*
199 *fischeri*. Expression of VF_0157 (*wbfB*), VF_0164 (*etp*), and VF_0165 (*wzc*) was

200 significantly higher in wild-type *V. fischeri* than in Δ*litR* (Table 2). Expression of *etp* was
201 significantly lower in Δ*hbtRC* constitutively expressing *hbtRC* compared to Δ*hbtRC*
202 carrying empty vector (Table 2), confirming that HbtR regulation of *litR* represses gene
203 expression in this locus.

204 Most of the genes in the locus VF_0157–80 are annotated as being involved in
205 production of extracellular polysaccharides. However, gene annotation alone could not
206 indicate which component(s) of the cell envelope (lipopolysaccharide O-antigen,
207 capsule, or exopolysaccharide (EPS)) might be affected by the genes in this locus. To
208 determine which polysaccharide type is produced by the enzymes encoded in
209 VF_0157–80, alcian blue staining was used to detect negatively charged
210 polysaccharides in the supernatants of liquid cultures of *V. fischeri* strains. Both Δ*litR*
211 and ΔVF0157–80 produced less alcian blue-staining EPS than wild-type *V. fischeri*, with
212 ΔVF_0157–80 producing even less EPS than Δ*litR* (Fig. 3). Overexpression of *hbtRC*
213 repressed EPS production in wild-type *V. fischeri*, but not in Δ*litR* or ΔVF_0157–80 (Fig.
214 3). Overexpression of *litR* in ΔVF_0157–80 did not complement the reduction in EPS
215 produced by that mutant (Fig. 3), indicating that essentially all EPS is produced by this
216 locus.

217

218 <u>*hbtRC* expression is regulated by Crp, but not by AphB or quorum sensing</u>. To
219 determine whether *hbtRC* expression in *V. fischeri* is affected by quorum sensing and/or
220 Crp, a regulator known to affect *tcpPH* expression in *V. cholerae*, RT-qPCR was
221 performed on wild-type *V. fischeri*, Δ*litR*, and Δ*crp* grown to OD_{600} ~0.3 and ~1.0.
222 Expression of *hbtRC* was lower at high cell density than at low cell density for all three

223 strains, with no difference between wild-type *V. fischeri* and Δ*litR* at either higher or
224 lower OD_{600} (Table 2). Expression of *hbtRC* in Δ*crp* was below that in wild-type *V.*
225 *fischeri* at low OD_{600}, but comparable at high OD_{600}. Thus, Crp appears to activate
226 *hbtRC* expression, the reverse of *tcpPH* regulation by Crp in *V. cholerae*.
227 Because Crp activates quorum-signaling genes in the *V. fischeri* genome (33,
228 34), we asked whether quorum signaling is responsible for the change in *hbtRC*
229 expression at different culture densities, and whether this regulation explains the lower
230 expression in the Δ*crp* mutant. The RT-qPCR experiment was repeated for wild-type *V.*
231 *fischeri* grown in SWT with or without added autoinducers. *hbtRC* expression remained
232 higher at lower cell density in the presence of both autoinducers (Table 2), indicating
233 that quorum signaling is not involved in Crp- and cell density-mediated *hbtRC*
234 regulation.
235 To determine whether the regulator AphAB and/or a change in pH affect *hbtRC*
236 expression in *V. fischeri*, RT-qPCR was performed on RNA extracted from cultures of
237 wild type or Δ*aphB V. fischeri* grown at pH 5.5 or 8.5. There was no significant
238 difference in *hbtRC* expression between any of the conditions (Table S2).
239
240 <u>*tcpPH* homologs do not cross-complement between *V. fischeri* and *V. cholerae*</u>. Δ*tcpPH*
241 and Δ*hbtRC* strains of *V. cholerae* and *V. fischeri*, respectively, were complemented
242 with empty vector, vector expressing *tcpPH*, or vector expressing *hbtRC*. RT-qPCR was
243 performed on RNA extracted from cultures of each strain to determine the level of *toxT*
244 expression in the *V. cholerae* strains or *litR* expression in the *V. fischeri* strains. While
245 expression of each *tcpPH* homolog complemented the respective deletion, cross-

246 complementation had no effect on output gene expression (Table S2), illustrating the
247 divergent activities of HbtR and TcpP.
248 In *V. cholerae*, ToxR cooperates with TcpP to activate *toxT* expression (35, 36),
249 begging the question of whether ToxR is also involved in controlling the *V. fischeri* HbtR
250 regulon. RT-qPCR performed on RNA extracted from cultures of Δ*hbtRC* and
251 Δ*hbtRC*Δ*toxRS* carrying either empty vector or vector expressing *hbtRC* showed that
252 *litR* expression was repressed to the same degree by HbtR regardless of the presence
253 or absence of *toxRS* (Table S2), further demonstrating that regulation by HbtR is
254 independent of ToxR and differs substantially from the TcpP system.
255
256 <u>Δ*hbtRC* has no defect in colonizing juvenile *E. scolopes* light organs.</u> Previous work
257 indicated that Δ*hbtRC* (then referred to as Δ*tcpPH*) had a light-organ colonization
258 defect, which appeared to increase through 96 h (19). We replicated this defect when
259 using the same conditions as the previous study (Fig. 4A); however, we observed an
260 advantage for Δ*hbtRC* when we reversed the fluorescent marker plasmids (Fig. 4A),
261 indicating the earlier results were due simply to experimental design. Co-colonization of
262 juvenile *E. scolopes* with chromosomally labeled strains resulted in no significant
263 colonization defect for either strain (Fig. 4B), demonstrating that HbtR is, in fact, not
264 required for entry into, or life inside, the *E. scolopes* light organ. Based on this
265 experience, we urge caution by other researchers using *rfp*-labeled pVSV208 in co-
266 colonization experiments.
267

268 Transcription of *hbtR* is activated as symbionts exit the light organ. Considering the
269 effects HbtR has on chemotaxis and luminescence gene expression (Tables 1, 2, and
270 S1), and that *hbtRC* has no effect on squid luminescence (Fig. S1) or colonization (Fig.
271 4B), we postulated that HbtR was likely to be involved in the transition into planktonic
272 life as *V. fischeri* exits the light organ. To establish at which point in the juvenile squid
273 diel cycle *V. fischeri hbtRC* expression is activated, we performed *in situ* hybridization
274 chain reaction (HCR) targeting *hbtR* mRNA to determine whether this gene was
275 expressed in the bacteria before, during, or after their expulsion from the squid light
276 organ into seawater. *hbtR* mRNA was not detected in *V. fischeri* cells within the crypts
277 or during expulsion along the path out of the light organ (Fig. 5A). Only in those cells
278 that had completely exited the light-organ pores was *hbtR* expression detected (Fig. 5B
279 and Movie S1). Within an hour of expulsion into seawater, ~25% of expelled *V. fischeri*
280 cells were expressing *hbtR* (Fig. 5C). As expected, transcripts of the quorum signaling-
281 induced gene *litR* were detected within *V. fischeri* cells inside the *E. scolopes* light-
282 organ crypts (Fig. S3); thus, it is unlikely that HCR was unable to detect *hbtR* transcripts
283 in colonizing bacteria due to failure of the reagents to penetrate the light organ.
284

285 **Discussion**

286 While much research has gone into understanding the mechanisms necessary for
287 colonization of the *E. scolopes* light organ by *V. fischeri* (reviewed most recently in
288 (37)), there has been little investigation into how the ~95% of symbiotic bacteria
289 expelled from the light organ at dawn each day transition back into life in seawater. In
290 this work we present HbtR, a heterofunctional homolog of the *V. cholerae* virulence

291 regulator TcpP that represses the quorum-signaling regulator LitR. While it is unclear at
292 this time whether HbtR represses *litR* expression directly or through some intermediate
293 regulator(s), the RNA-seq data indicate HbtR does not act through a step in the
294 quorum-signaling pathway upstream of LitR (Table S1). Through the discovery of
295 additional functions regulated by LitR, namely chemotaxis, motility, and EPS production,
296 we have begun to build a picture in which LitR aids the transition by *V. fischeri* into a
297 colonization lifestyle and, upon expulsion from the light organ, HbtR reverses that
298 process to help transition back into planktonic life (Fig. 6). This is a markedly different
299 role for HbtR from that of TcpP.

300 The regulatory mechanisms controlling *hbtRC* expression, as elucidated thus far,
301 are similar to the *tcpPH* regulatory pathway in *V. cholerae* only in that both operons are
302 regulated by the global regulator Crp, albeit in the opposite manner. Notably, the *hapR*
303 homolog in *V. fischeri*, *litR*, is itself repressed by HbtR (Tables 1, S1, S2), a reversal of
304 roles from those in *V. cholerae*. Considering the distinct regulatory pathways for HbtR
305 and TcpP, as well as the low percent identity (26.8%) of the two protein sequences, it
306 appears, evolutionarily, that either progenitors of *tcpPH* and *hbtRC* were acquired
307 independently after separation of the two species' ancestors, or the parent operon
308 evolved in dramatically different fashions as the two species evolved to inhabit disparate
309 environmental niches. Determining which of these histories is the more likely is beyond
310 the scope of this study, but in either case it is clear the two homologs have been
311 recruited into specialized roles befitting the two species' distinct lifestyles, i.e.,
312 pathogenesis versus beneficial symbiosis within animal hosts.

313 The data presented here suggest HbtR acts as a first-wave responder as *V.*
314 *fischeri* bacteria exit the light organ and re-enter the seawater (Fig. 5), a significant
315 change in environmental conditions and an imperative for survival. This role could
316 explain some of the discrepancies observed between the RNA-seq results in the
317 present study and those in Thompson 2017 (19). For example, the Thompson data
318 indicate that in addition to *hbtR* and *hbtC*, the luminescence genes *luxR*, *luxI*, and
319 *luxCDABEG* were also highly upregulated in cells recently expelled from the light
320 organs compared to planktonic cells, while *litR*, which activates the *lux* genes, was not
321 differentially regulated between the two cell populations. Meanwhile, the results of this
322 study indicate that HbtR represses LitR and consequently causes the downregulation of
323 *lux* and other downstream quorum-signaling genes (Tables 1, S1, S2). Similarly, the
324 gene most highly upregulated by HbtR in the RNA-seq data presented here was
325 VF_2042 (Table S1), one of the four MCP genes repressed by LitR (Table 2); in the
326 earlier study, VF_2042 was downregulated in cells released from the light organs (19).
327 These results are consistent with a model in which HbtR becomes active once *V.*
328 *fischeri* exits the light organ, with some of the earliest effects seen in its repression of
329 *litR*. In the earlier study, it may have been that in the ~25 minutes between initiation of
330 light-organ expulsion and harvesting the *V. fischeri* RNA, HbtR had become activated
331 (Fig. 5) and was already repressing *litR* expression, but the downstream effects (e.g.,
332 on VF_2042 and *lux* gene expression) were not yet apparent.
333 Previous studies have also demonstrated a repression of several flagellin genes
334 by AinS and increased motility in a *litR* mutant (31). Here we show that LitR represses
335 numerous flagellin, motor, and chemotaxis genes, including at least two MCP genes

336 involved in chemotaxis toward $(GlcNAc)_2$, an *N*-acetylated sugar reported to be an
337 important chemoattractant during light-organ colonization (12). Previous work indicated
338 that a *litR* mutant colonized *E. scolopes* to a lower level than wild-type *V. fischeri* (31),
339 which the authors suggested was due to an initiation delay due to hypermotility.
340 However, in the study in which LitR was first described (4), a *litR* mutant had an
341 advantage in initiating light-organ colonization over wild-type *V. fischeri.* Based on work
342 presented here, including a demonstration that MCP genes repressed by LitR are
343 involved in light-organ colonization (Fig. 2), we posit that the *litR*-mutant colonization
344 benefit (4) may have resulted from the increase in both motility and chemotaxis into the
345 light organ by that mutant. We hypothesize that the lower level of colonization observed
346 for the *litR* mutant in single-strain experiments (31) may have been due to dysregulation
347 of a separate symbiotic process, perhaps extracellular polysaccharide production.
348 LitR appears to activate, and HbtR to thus repress, a large locus of genes
349 (VF_0157–80) involved in extracellular polysaccharide production (Tables 1, S1, S2).
350 Fidopiastis et al. (4) noted that *litR*$^-$ colonies are less opaque than wild-type *V. fischeri*
351 and suggested this phenotype may be due to a difference in the extracellular
352 polysaccharides present in each strain. The nature of polysaccharide affected by
353 VF_0157–80 is not fully established, yet it seems most likely to be an EPS, or “slime
354 layer,” due to the ease with which it separates from the bacterial cell during
355 centrifugation (Fig. 3A). While lipopolysaccharide and the *syp* polysaccharide have
356 been implicated in the initiation of host colonization by *V. fischeri* (38–40), little has been
357 determined regarding the possible involvement of extracellular polysaccharides in
358 colonization persistence. *V. fischeri*-colonized crypts, despite having no goblet cells

359 (Nyholm, personal communication), have been shown to stain alcian blue-positive (41),
360 indicating that the presumptive EPS made by VF_0157–80 may be a relevant factor in
361 *E. scolopes*-*V. fischeri* symbiosis. This aspect of the symbiotic relationship could have
362 broader implications for host-microbe interactions in general.
363

364 **Materials and Methods**

365 **Bacterial strains and growth conditions.** Bacterial strains and plasmids used in this
366 study are summarized in Table S3. *E. coli* and *V. cholerae* were grown in lysogeny
367 broth (LB; (42), (19)) at 37°C; *V. fischeri* was grown in LB-salt (LBS; (43)) at 28°C.
368 Overnight cultures were inoculated with single colonies from freshly streaked -80°C
369 stocks. Liquid cultures were shaken at 225 rpm. Unless otherwise noted, 15 g of agar
370 were added per liter for solid media. Antibiotics were added to overnight cultures, where
371 applicable, at the following concentrations: kanamycin (Km), 50 µg/mL; chloramphenicol
372 (Cm), 5 µg/mL (*V. fischeri*) or 25 µg/mL (*E. coli*). Experimental cultures were grown in
373 either seawater-tryptone (SWT) medium (44) or minimal-salts medium (MSM; per L: 8.8
374 g NaCl, 6.2 g $MgSO_4 \cdot 7H_2O$, 0.74 g $CaCl_2 \cdot 2H_2O$, 0.0204 g H_2NaPO_4, 0.37 g KCl, 8.66 g
375 PIPES disodium salt, 0.65 mg $FeSO_4 \cdot 7H_2O$; pH 7.5) supplemented with 5 mg/L
376 casamino acids and a carbon source as indicated. The results of all experiments are
377 reported as the means of three (or more, as indicated) biological replicates ± 1 standard
378 deviation (SD). Statistical analysis was performed using Welch's t-test.

379 **Plasmid and mutant construction.** Primers used to construct the deletion and
380 expression vectors in this study are listed in Table S4. In-frame deletion of genes from
381 the *V. fischeri* genome was performed as previously described (45, 46). Counter-

382 selection to remove the target gene and pSMV3 was performed on LB-sucrose (per L:
383 2.5 g NaCl, 10 g Bacto Tryptone, 5 g yeast extract, 100 g sucrose) for two days at room
384 temperature. Expression vectors were constructed by amplifying and ligating the target
385 gene into the multiple cloning site of pVSV105 (47). Inducible expression of *hbtRC* was
386 achieved by ligating *lacI*^{q} from pAKD601 to *hbtRC* cloned from the *V. fischeri* genome
387 and inserting the fusion into the multiple cloning site of pVSV105. Overexpression of
388 *hbtRC* brought the level of expression closer to that found upon expulsion from juvenile
389 squid (19), which was higher than we measured for wild-type *V. fischeri* in culture
390 conditions. Genomic insertion of *gfp* or *rfp* under control of the *lac* promoter at the
391 *attTn7* site was performed using a mini-Tn7 vector as described (48). Previously
392 constructed Δ*hbtRC* (19) was used to recapitulate conditions for follow-up on previous
393 experiments (RNA-seq and squid co-colonization); a newly derived Δ*hbtRC* strain was
394 used for all other experiments so it would have the same parent wild-type *V. fischeri*
395 stock as other mutants created in this study.
396 **Generation and analysis of RNAseq libraries.** RNA extraction and RNAseq were
397 performed as previously described (19). Briefly, RNA was stabilized with RNAprotect
398 Bacterial Reagent (Qiagen) and extracted with an RNeasy Mini Kit (Qiagen) from 500
399 µL of cultures grown to mid-log phase in SWT with 1.75 mM IPTG. RNA was extracted
400 from biological triplicates for each strain. Contaminating DNA was degraded by
401 treatment with TURBO DNase (Invitrogen). Ribosomal reduction, strand-specific library
402 preparation, and paired-end 50-bp sequence analysis on an Illumina HiSeq 2500 on
403 high-output mode were performed at the University of Minnesota Genomics Center.
404 Sequences were processed on the open-source Galaxy server (usegalaxy.org; (49))

405 using the following workflow (default settings used unless otherwise indicated): reads
406 were trimmed with Trimmomatic (maximum mismatch:1, LEADING:3, TRAILING:3,
407 SLIDINGWINDOW:4,20, MINLEN:35), mapped to the *V. fischeri* chromosomes and
408 plasmid (accession nos. NC_006840.2, NC_006841.2, and NC_006842.2) using
409 Bowtie2 (-un-con, --sensitive), and counted with featureCounts (-p
410 disabled, -t=gene, -g=locus_tag, -Q=10, -s); differential expression was analyzed with
411 DESeq2 (outliers filtering and independent filtering turned on). Between 11.7 million and
412 12.7 million paired reads were mapped to the *V. fischeri* genome per biological
413 replicate. Raw and processed read files have been deposited into the NCBI Gene
414 Expression Omnibus server (GSE151621).
415 **Reverse transcription and quantitative PCR.** RNA from bacterial cultures was
416 extracted as described above and treated with TURBO DNase (Invitrogen). cDNA was
417 synthesized from DNase-treated RNA using SMART MMLV Reverse Transcriptase
418 (Clontech) and Random Hexamer Primer (Thermo Scientific). Gene expression was
419 measured by qPCR performed with LightCycler 480 SYBR Green I Master Mix (Roche)
420 under the following conditions: 95°C for 5 min; 45 cycles of 95°C for 10 sec, 60°C for 20
421 sec, and 72°C for 20 sec; melting curve acquisition from 65°C to 97°C. qPCR primer
422 pairs were designed for these conditions and confirmed to have efficiencies between 90
423 and 110%. Cycle thresholds (Ct) for each sample were normalized to those of the
424 reference gene *polA* (ΔCt = target gene-*polA*; *polA* expression primers provided
425 courtesy of Silvia Moriano-Gutierrez). ΔΔCt values were calculated by subtracting the
426 average ΔCt for the parent strain, at higher pH or lower OD_{600} when appropriate; fold
427 changes were calculated as $2^{(-\Delta\Delta Ct)}$.

428 **Growth and luminescence curves.** Overnight LBS cultures of each strain were
429 pelleted, washed once, and resuspended in 1 mL of the intended growth medium.
430 Luminescence growth curves were performed in 20 mL SWT in flasks shaking at 225
431 rpm; periodic 1 mL and 300 µL aliquots were taken for luminescence and OD_{600}
432 readings on a luminometer (Turner Designs) and Tecan Genios plate reader,
433 respectively. Growth curves were performed in 1.2 mL growth medium and monitored in
434 the Tecan Genios plate reader with continuous shaking at high speed.
435 **Squid colonization assays.** Juvenile squid colonization experiments were performed
436 as described previously (50), with juvenile squid exposed to *V. fischeri* strains at 1,000–
437 6,000 CFU/mL either for 3 h or overnight, as indicated, before being placed in fresh
438 sterile seawater until euthanizing by freezing. Colonization competition experiments
439 were performed by exposing juvenile squid to a 1:1 inoculum of each strain.
440 ***In situ* hybridization chain reaction.** HCR (51) was performed on squid colonized with
441 wild-type *V. fischeri* carrying a *gfp*-labeled plasmid and on *V. fischeri* cells 1 h after
442 being expelled from squid light organs as previously described (52–54). Briefly, *E.*
443 *scolopes* juveniles and expelled *V. fischeri* cells were fixed in 4% paraformaldehyde in
444 marine phosphate-buffered saline either before or after a light cue stimulated bacterial
445 expulsion. HCR was performed on dissected light organs (52) and expelled *V. fischeri*
446 cells affixed to gelatin-coated slides (adapted from (53)) using HCR version 3.0
447 chemistry (54). Ten probes targeting *hbtR* mRNA and eleven probes targeting *litR*
448 mRNA (Table 3) were amplified with Alexa Fluor 546-labeled hairpins (Molecular
449 Instruments). Light organs were then counterstained overnight with a 1:750 dilution of
450 4′,6-diamidino-2-phenylindole (DAPI; Thermo Fisher Scientific) in 5x SSC-Tween before

451 mounting on slides with Vectashield (Vector Laboratories) and overlaid with a coverslip
452 (#1.5, Fisherbrand, Fisher Scientific). Imaging was done on an upright Zeiss LSM 710
453 laser-scanning confocal microscope at the University of Hawai‘i Kewalo Marine
454 Laboratory; images were analyzed using FIJI (ImageJ) (55).
455 **Motility and chemotaxis assays.** Soft-agar motility assays were performed as
456 previously described (56). Briefly, the equivalent of 10 µL of a bacterial culture grown to
457 an OD_{600} of 0.5 in SWT were spotted onto minimal-medium plates containing 0.25%
458 agar and, when appropriate, 1 mM chemoattractant. Migration zones were measured
459 after 18–24 h of static incubation at 28°C.
460 **Alcian blue detection of extracellular polysaccharides.** EPS was detected by
461 staining with alcian blue essentially as previously described (57). Single colonies from
462 freshly streaked -80°C stocks were used to inoculate MSM supplemented with 6.5 mM
463 Neu5Ac and 0.05% (wt/vol) casamino acids and grown with shaking 18–22 h. EPS was
464 separated from cells by centrifugation of the equivalent of 2.5 mL at OD_{600}=1.0 for 15
465 min at 12,000 xg and 4°C. 250 µL of this supernatant was mixed with 1 mL alcian-blue
466 solution (per L: 0.5 g alcian blue, 30 mL glacial acetic acid, pH 2.5) and rocked for 1 h at
467 room temperature, then centrifuged for 10 min at 10,000 rpm and 4°C. Pellets were
468 resuspended in 1 mL 100% ethanol, then centrifuged for 10 min at 10,000 xg and 4°C.
469 Pellets were solubilized in 500 µL SDS (per L: 100 g sodium dodecyl sulfate, 50 mM
470 sodium acetate, pH 5.8), and the absorbance was read at OD_{620}.
471
472 **Acknowledgments**

The authors thank Silvia Moriano-Gutierrez and Alexandrea Duscher for advice regarding RNA-seq, Elliott McCloskey and Roxane Gaedeke for help with experiment execution, the University of Minnesota Genomics Center for RNA processing and next-generation sequencing, and the Ruby and McFall-Ngai laboratories for their insights. The research was supported by NIH grants R37 AI50661 (Margaret McFall-Ngai and E.G.R.), R01 OD11024, and R01 GM135254 (E.G.R. and M.M.-N.) and NSF INSPIRE Grant MCB1608744 (Eva Kanso and Scott Fraser, University of Southern California). Acquisition of the Leica TCS SP8 X confocal was supported by NSF DBI 1828262 (Marilyn Dunlap, E.G.R., and M.M.-N.), and microscopy was performed in the MICRO facility, supported by COBRE P20 GM125508 (M.M.-N. and E.G.R.).

References

1. Eberhard A, Burlingame AL, Eberhard C, Kenyon GL, Nealson KH, Oppenheimer NJ. 1981. Structural identification of autoinducer of *Photobacterium fischeri* luciferase. Biochemistry 20:2444–2449.

2. Kuo A, Blough NV, Dunlap PV. 1994. Multiple N-acyl-L-homoserine lactone autoinducers of luminescence in the marine symbiotic bacterium *Vibrio fischeri*. J Bacteriol 176:7558–7565.

3. Eberhard A. 1972. Inhibition and activation of bacterial luciferase synthesis. J Bacteriol 109:1101–1105.

4. Fidopiastis PM, Miyamoto CM, Jobling MG, Meighen EA, Ruby EG. 2002. LitR, a new transcriptional activator in *Vibrio fischeri*, regulates luminescence and symbiotic light organ colonization. Mol Microbiol 45:131–143.

5. Engebrecht J, Silverman M. 1984. Identification of genes and gene products necessary for bacterial bioluminescence. Proc Natl Acad Sci U S A 81:4154–4158.

6. Verma SC, Miyashiro T. 2013. Quorum Sensing in the squid-vibrio symbiosis. Int J Mol Sci 14:16386–16401.

7. Visick KL, Foster J, Doino J, McFall-Ngai M, Ruby EG. 2000. *Vibrio fischeri lux* genes play an important role in colonization and development of the host light organ. J Bacteriol 182:4578–4586.

503 8. Koch EJ, Miyashiro T, McFall-Ngai MJ, Ruby EG. 2014. Features governing
504 symbiont persistence in the squid-vibrio association. Mol Ecol 23:1624–1634.

505 9. Moriano-Gutierrez S, Koch EJ, Bussan H, Romano K, Belcaid M, Rey FE, Ruby
506 EG, McFall-Ngai MJ. 2019. Critical symbiont signals drive both local and systemic
507 changes in diel and developmental host gene expression. Proc Natl Acad Sci U S A
508 116:7990–7999.

509 10. Wei SL, Young RE. 1989. Development of symbiotic bacterial bioluminescence in
510 a nearshore cephalopod, *Euprymna scolopes*. Mar Biol 103:541–546.

511 11. Graf J, Dunlap PV, Ruby EG. 1994. Effect of transposon-induced motility
512 mutations on colonization of the host light organ by *Vibrio fischeri*. J Bacteriol
513 176:6986–6991.

514 12. Mandel MJ, Schaefer AL, Brennan CA, Heath-Heckman EAC, Deloney-Marino
515 CR, McFall-Ngai MJ, Ruby EG. 2012. Squid-derived chitin oligosaccharides are a
516 chemotactic signal during colonization by *Vibrio fischeri*. Appl Environ Microbiol
517 78:4620–4626.

518 13. Ruby EG, Asato LM. 1993. Growth and flagellation of *Vibrio fischeri* during
519 initiation of the sepiolid squid light organ symbiosis. Arch Microbiol 159:160–167.

520 14. Graf J, Ruby EG. 1998. Host-derived amino acids support the proliferation of
521 symbiotic bacteria. Proc Natl Acad Sci U S A 95:1818–1822.

522 15. Jones BW, Nishiguchi MK. 2004. Counterillumination in the Hawaiian bobtail
523 squid, *Euprymna scolopes* Berry (Mollusca: Cephalopoda). Mar Biol 144:1151–1155.

524 16. Stabb EV, Millikan DS, Millikan DS. 2009. Is the *Vibrio fischeri–Euprymna*
525 *scolopes* symbiosis a defensive mutualism? *In* Defensive Mutual Microb Symbiosis.
526 CRC Press.

527 17. Lee K-H, Ruby EG. 1994. Effect of the squid host on the abundance and
528 distribution of symbiotic *Vibrio fischeri* in nature. Appl Environ Microbiol 60:1565–1571.

529 18. Nyholm SV, McFall-Ngai MJ. 1998. Sampling the light-organ microenvironment
530 of *Euprymna scolopes*: description of a population of host cells in association with the
531 bacterial symbiont *Vibrio fischeri*. Biol Bull 195:89–97.

532 19. Thompson LR, Nikolakakis K, Pan S, Reed J, Knight R, Ruby EG. 2017.
533 Transcriptional characterization of *Vibrio fischeri* during colonization of juvenile
534 *Euprymna scolopes*. Environ Microbiol 19:1845–1856.

535 20. Thomas S, Williams SG, Manning PA. 1995. Regulation of *tcp* genes in classical
536 and El Tor strains of *Vibrio cholerae* O1. Gene 166:43–48.

537 21. Häse CC, Mekalanos JJ. 1998. TcpP protein is a positive regulator of virulence
538 gene expression in *Vibrio cholerae*. Proc Natl Acad Sci U S A 95:730–734.

539 22. Taylor RK, Miller VL, Furlong DB, Mekalanos JJ. 1987. Use of *phoA* gene fusions
540 to identify a pilus colonization factor coordinately regulated with cholera toxin. Proc Natl
541 Acad Sci U S A 84:2833–2837.

542 23. Skorupski K, Taylor RK. 1999. A new level in the *Vibrio cholerae* ToxR virulence
543 cascade: AphA is required for transcriptional activation of the *tcpPH* operon. Mol
544 Microbiol 31:763–771.

545 24. Kovacikova G, Skorupski K. 1999. A *Vibrio cholerae* LysR homolog, AphB,
546 cooperates with AphA at the *tcpPH* promoter to activate expression of the ToxR
547 virulence cascade. J Bacteriol 181:4250–4256.

548 25. Kovacikova G, Lin W, Skorupski K. 2010. The LysR-type virulence activator
549 AphB regulates the expression of genes in *Vibrio cholerae* in response to low pH and
550 anaerobiosis. J Bacteriol 192:4181–4191.

551 26. Zhu J, Miller MB, Vance RE, Dziejman M, Bassler BL, Mekalanos JJ. 2002.
552 Quorum-sensing regulators control virulence gene expression in *Vibrio cholerae*. Proc
553 Natl Acad Sci U S A 99:3129–3134.

554 27. Kovacikova G, Skorupski K. 2002. Regulation of virulence gene expression in
555 *Vibrio cholerae* by quorum sensing: HapR functions at the *aphA* promoter. Mol Microbiol
556 46:1135–1147.

557 28. Kovacikova G, Skorupski K. 2001. Overlapping binding sites for the virulence
558 gene regulators AphA, AphB and cAMP-CRP at the *Vibrio cholerae tcpPH* promoter.
559 Mol Microbiol 41:393–407.

560 29. Larocque RC, Harris JB, Dziejman M, Li X, Khan AI, Faruque ASG, Faruque SM,
561 Nair GB, Ryan ET, Qadri F, Mekalanos JJ, Calderwood SB. 2005. Transcriptional
562 profiling of *Vibrio cholerae* recovered directly from patient specimens during early and
563 late stages of human infection. Infect Immun 73:4488–4493.

564 30. Schild S, Tamayo R, Nelson EJ, Qadri F, Calderwood SB, Camilli A. 2007.
565 Genes induced late in infection increase fitness of *Vibrio cholerae* after release into the
566 environment. Cell Host Microbe 2:264–277.

567 31. Lupp C, Ruby EG. 2005. *Vibrio fischeri* uses two quorum-sensing systems for the
568 regulation of early and late colonization factors. J Bacteriol 187:3620–3629.

569 32. Cao X, Studer SV, Wassarman K, Zhang Y, Ruby EG, Miyashiro T. 2012. The
570 novel sigma factor-like regulator RpoQ controls luminescence, chitinase activity, and
571 motility in *Vibrio fischeri*. mBio e00285-11

572 33. Dunlap PV, Greenberg EP. 1985. Control of *Vibrio fischeri* luminescence gene
573 expression in *Escherichia coli* by cyclic AMP and cyclic AMP receptor protein. J
574 Bacteriol 164:45–50.

575 34. Lyell NL, Colton DM, Bose JL, Tumen-Velasquez MP, Kimbrough JH, Stabb EV.
576 2013. Cyclic AMP receptor protein regulates pheromone-mediated bioluminescence at
577 multiple levels in *Vibrio fischeri* ES114. J Bacteriol 195:5051–5063.

578 35. Murley YM, Carroll PA, Skorupski K, Taylor RK, Calderwood SB. 1999.
579 Differential transcription of the *tcpPH* operon confers biotype-specific control of the
580 *Vibrio cholerae* ToxR virulence regulon. Infect Immun 67:5117–5123.

581 36. Krukonis ES, Yu RR, Dirita VJ. 2000. The *Vibrio cholerae* ToxR/TcpP/ToxT
582 virulence cascade: distinct roles for two membrane-localized transcriptional activators
583 on a single promoter. Mol Microbiol 38:67–84.

584 37. Norsworthy AN, Visick KL. 2013. Gimme shelter: how *Vibrio fischeri* successfully
585 navigates an animal's multiple environments. Front Microbiol 4:356.

586 38. Yip ES, Grublesky BT, Hussa EA, Visick KL. 2005. A novel, conserved cluster of
587 genes promotes symbiotic colonization and σ^{54} -dependent biofilm formation by *Vibrio*
588 *fischeri*: *syp*, a novel symbiosis locus in *Vibrio fischeri*. Mol Microbiol 57:1485–1498.

589 39. Post DM, Yu L, Krasity BC, Choudhury B, Mandel MJ, Brennan CA, Ruby EG,
590 McFall-Ngai MJ, Gibson BW, Apicella MA. 2012. O-antigen and core carbohydrate of
591 *Vibrio fischeri* lipopolysaccharide: composition and analysis of their role in *Euprymna*
592 *scolopes* light organ colonization. J Biol Chem 287:8515-30.

593 40. Schwartzman JA, Lynch JB, Flores Ramos S, Zhou L, Apicella MA, Yew JY,
594 Ruby EG. 2019. Acidic pH promotes lipopolysaccharide modification and alters
595 colonization in a bacteria-animal mutualism. Mol Microbiol 112:1326–1338.

596 41. Nyholm SV, Deplancke B, Gaskins HR, Apicella MA, McFall-Ngai MJ. 2002.
597 Roles of *Vibrio fischeri* and nonsymbiotic bacteria in the dynamics of mucus secretion
598 during symbiont colonization of the *Euprymna scolopes* light organ. Appl Environ
599 Microbiol 68:5113–5122.

600 42. Bertani G. 1951. Studies on lysogenesis. I. The mode of phage liberation by
601 lysogenic *Escherichia coli*. J Bacteriol 62:293–300.

602 43. Stabb EV, Reich KA, Ruby EG. 2001. *Vibrio fischeri* genes *hvnA* and *hvnB*
603 encode secreted NAD+-glycohydrolases. J Bacteriol 183:309–317.

604 44. Boettcher KJ, Ruby EG. 1990. Depressed light emission by symbiotic *Vibrio*
605 *fischeri* of the sepiolid squid *Euprymna scolopes*. J Bacteriol 172:3701–3706.

606 45. Saltikov CW, Newman DK. 2003. Genetic identification of a respiratory arsenate
607 reductase. Proc Natl Acad Sci U S A 100:10983–10988.

608 46. Bennett BD, Redford KE, Gralnick JA. 2018. Survival of anaerobic Fe^{2+} stress
609 requires the ClpXP protease. J Bacteriol 200:e00671-17.

610 47. Dunn AK, Millikan DS, Adin DM, Bose JL, Stabb EV. 2006. New *rfp*- and
611 pES213-derived tools for analyzing symbiotic *Vibrio fischeri* reveal patterns of infection
612 and *lux* expression *in situ*. Appl Environ Microbiol 72:802–810.

613 48. McCann J, Stabb EV, Millikan DS, Ruby EG. 2003. Population dynamics of *Vibrio*
614 *fischeri* during Infection of *Euprymna scolopes*. Appl Environ Microbiol 69:5928–5934.

615 49. Afgan E, Baker D, Batut B, van den Beek M, Bouvier D, Cech M, Chilton J,
616 Clements D, Coraor N, Grüning BA, Guerler A, Hillman-Jackson J, Hiltemann S, Jalili V,
617 Rasche H, Soranzo N, Goecks J, Taylor J, Nekrutenko A, Blankenberg D. 2018. The
618 Galaxy platform for accessible, reproducible and collaborative biomedical analyses:
619 2018 update. Nucleic Acids Res 46:W537–W544.

620 50. Bongrand C, Ruby EG. 2019. Achieving a multi-strain symbiosis: strain behavior
621 and infection dynamics. ISME J 13:698-706.

622 51. Choi HMT, Chang JY, Trinh LA, Padilla JE, Fraser SE, Pierce NA. 2010.
623 Programmable *in situ* amplification for multiplexed imaging of mRNA expression. Nat
624 Biotechnol 28:1208–1212.

625 52. Nikolakakis K, Lehnert E, McFall-Ngai MJ, Ruby EG. 2015. Use of hybridization
626 chain reaction-fluorescent *in situ* hybridization to track gene expression by both partners
627 during initiation of symbiosis. Appl Environ Microbiol 81:4728–4735.

628 53. Choi HMT, Calvert CR, Husain N, Huss D, Barsi JC, Deverman BE, Hunter RC,
629 Kato M, Lee SM, Abelin ACT, Rosenthal AZ, Akbari OS, Li Y, Hay BA, Sternberg PW,
630 Patterson PH, Davidson EH, Mazmanian SK, Prober DA, van de Rijn M, Leadbetter JR,
631 Newman DK, Readhead C, Bronner ME, Wold B, Lansford R, Sauka-Spengler T, Fraser
632 SE, Pierce NA. 2016. Mapping a multiplexed zoo of mRNA expression. Dev Camb Engl
633 143:3632–3637.

634 54. Choi HMT, Schwarzkopf M, Fornace ME, Acharya A, Artavanis G, Stegmaier J,
635 Cunha A, Pierce NA. 2018. Third-generation *in situ* hybridization chain reaction:
636 multiplexed, quantitative, sensitive, versatile, robust. Development 145:dev165753.

637 55. Schindelin J, Arganda-Carreras I, Frise E, Kaynig V, Longair M, Pietzsch T,
638 Preibisch S, Rueden C, Saalfeld S, Schmid B, Tinevez J-Y, White DJ, Hartenstein V,
639 Eliceiri K, Tomancak P, Cardona A. 2012. Fiji: an open-source platform for biological-
640 image analysis. Nat Methods 9:676–682.

641 56. DeLoney-Marino CR. 2013. Observing chemotaxis in *Vibrio fischeri* using soft
642 agar assays in an undergraduate microbiology laboratory. J Microbiol Biol Educ JMBE
643 14:271–272.

644 57. Plante C. 2000. Role of bacterial exopolymeric capsules in protection from
645 deposit-feeder digestion. Aquat Microb Ecol 21:211–219.

646

647 **FIGURE LEGENDS**

648

649 **FIG 1** Luminescence and growth of wild-type *V. fischeri* and Δ*hbtRC* strains. The rates
650 of (A) light production and (B) growth in SWT were measured for wild-type *V. fischeri*
651 (circles) and Δ*hbtRC* (squares) carrying empty pVSV105 (open symbols) or
652 pVSV105::*hbtRC* (closed symbols). Results represent the means of three biological
653 replicates ± one standard deviation. RLU, relative light units; Abs, absorbance.

654

655 **FIG 2** Light-organ colonization competition between wild-type *V. fischeri* and a
656 chemotaxis mutant. Ratios of wild-type *V. fischeri* (WT) carrying a GFP-encoding
657 plasmid (pVSV102) vs. unlabeled ΔVF_1133 ΔVF_2042 ΔVF_A0246 ΔVF_A0389
658 ("ΔΔΔΔ") (circles) or unlabeled wild-type *V. fischeri* vs. ΔΔΔΔ carrying pVSV102
659 (squares) colonizing juvenile *E. scolopes* light organs were measured after 3 h of
660 exposure to the inoculum followed by 21 h of incubation in sterile seawater. RCI,
661 relative competitive index of bacterial strains. Each point represents one animal. Empty
662 symbols represent the limit of detection for light organs in which only the wild-type strain
663 was found. Error bars represent ± one standard deviation.

664

665 **FIG 3** EPS production in wild-type *V. fischeri*, Δ*litR*, and ΔVF_0157–80 strains. EPS in
666 supernatants of 24-h cultures grown in 0.05% casamino acids and 6.5 mM Neu5Ac was
667 stained with alcian blue for wild-type *V. fischeri* (circles), Δ*litR* (squares), and
668 ΔVF_0157–80 (triangles) carrying empty pVSV105 (open symbols), pVSV105::*hbtRC*
669 (half-filled symbols), or pVSV105::*litR* (closed symbols). Error bars represent ± one

670 standard deviation. Abs, absorbance.*, $p<0.05$; **, $p<0.005$; ***, $p<0.001$; n.s., not
671 statistically significant.
672
673 **FIG 4** Light-organ colonization competition between wild-type *V. fischeri* and Δ*hbtRC*
674 strains. (A) Ratios of wild-type *V. fischeri* carrying a GFP-encoding plasmid (pVSV102)
675 vs. Δ*hbtRC* carrying an RFP-encoding plasmid (pVSV208) (circles, squares, and
676 triangles) or wild-type *V. fischeri* (WT) carrying pVSV208 vs. Δ*hbtRC* carrying pVSV102
677 (diamonds) colonizing juvenile *E. scolopes* light organs were measured after 1 to 10 d.
678 (B) Ratios of wild-type *V. fischeri* with chromosomal *gfp* vs. Δ*hbtRC* with chromosomal
679 *rfp* (squares) or wild-type *V. fischeri* with chromosomal *rfp* vs. Δ*hbtRC* with
680 chromosomal *gfp* (circles) colonizing juvenile *E. scolopes* light organs were measured
681 after 1 d. RCI, relative competitive index of bacterial strains. Each point represents one
682 animal. Empty symbols represent the limit of detection for light organs in which only the
683 *gfp*-carrying strain was found. Error bars represent ± one standard deviation. n.s., not
684 statistically significant.
685
686 **FIG 5** Expression of *hbtR* in *V. fischeri* during expulsion from *E. scolopes* light organs.
687 Transcripts of *hbtR* (magenta, arrowheads) were detected using *in situ* HCR in *V.*
688 *fischeri* cells (green) during expulsion from *E. scolopes* juvenile light organ crypts. (A) *V.*
689 *fischeri* symbionts originate in the crypt, pass through the migration path (mp), and exit
690 through the external surface pore; (A) merged image, (A') GFP channel, (A") *hbtR*
691 transcript channel (Alexa 546). (B) *V. fischeri* cells (green) are expelled through the
692 external surface pore (asterisk) into seawater 1 h after a dawn light cue; (B) a single

693 optical slice of the superficial layer above the exit point from host and *V. fischeri* cells
694 outside of the pore expressing *hbtR*; (B'), the corresponding merged composite stack
695 (video in Movie S1). (C) One hour after expulsion into ambient seawater, vented cells
696 express *hbtR* (magenta); enlargement is of the area within the dashed square. (C')
697 Percentage and 95% confidence intervals of vented cells expressing *hbtR* calculated
698 from four samples of ventate on slides, from two experiments. Blue, *E. scolopes* nuclei
699 (DAPI).
700
701 **FIG 6** Model proposing regulation by HbtR and LitR in *V. fischeri* during colonization of
702 and expulsion from the *E. scolopes* light organ. Upon colonization, LitR regulates
703 relevant physiological phenotypes, including activation of luminescence and EPS
704 production and repression of motility and chemotaxis. HbtR causes the repression of
705 *litR* expression upon expulsion of *V. fischeri* from the light organ, reversing this process
706 and leading to the upregulation of motility and chemotaxis and the downregulation of
707 luminescence and EPS production. Gray text, downregulated genes and phenotypes;
708 blue text, upregulated genes and phenotypes.
709

710 **SUPPLEMENTAL MATERIAL LEGENDS**

711 **FIG S1** Luminescence of wild-type *V. fischeri* and Δ*hbtRC* strains during symbiosis.
712 Luminescence was measured in juvenile squid 24 h or 48 h after colonization with either
713 wild-type *V. fischeri* (●) or Δ*hbtRC* (■). Each point represents one animal. Mean values
714 indicated; no significant differences were noted between strains at either time-point.
715 RLU, relative light units.

716 **FIG S2** Growth of wild-type *V. fischeri* and chemotaxis mutants on *N*-acetylated sugars.
717 (A) The rates of growth in MSM supplemented with 0.05% casamino acids and 6.5 mM
718 Neu5Ac were measured for wild-type *V. fischeri* (●), ΔΔΔΔ (■), and ΔVF_1133
719 ΔVF_A0246 (▲). (B) The rates of growth in MSM supplemented with 0.05% casamino
720 acids and 6.5 mM GlcNAc were measured for wild-type *V. fischeri* (●) and ΔΔΔΔ (■).
721 Results represent means of three biological replicates ± one standard deviation. Abs,
722 absorbance.
723

724 **FIG S3** Expression of *litR* in *V. fischeri* when host-associated within the *E. scolopes* light
725 organ. Transcripts of *litR* (green) were detected using *in situ* HCR in *V. fischeri* cells
726 colonizing *E. scolopes* crypts (C) after traversing the tissues of the migration path (MP).
727 Blue, *E. scolopes* nuclei (DAPI); green, *litR* transcripts (Alexa 546). Bar 15 μm.
728

729 **TABLE S1 RNA-seq data file** Expression-level counts of all orfs in the *V. fischeri*
730 genome. Comparison of mapped read counts for Δ*hbtRC* and *hbtRC* (induced)
731

732 **TABLE S2 RT-qPCR results**
733

734 **TABLE S3 Bacterial strains and plasmids used in this work**
735

736 **TABLE S4 Primers and probes used in this work**

737

738 **MOVIE S1** Expression of *hbtR* in *V. fischeri* cells during their expulsion from an *E.*
739 *scolopes* light organ. *hbtR* transcripts were detected using *in situ* HCR in *V. fischeri*
740 cells expelled from the external surface pore of the light organ 1 h after a dawn light
741 cue. Merged stack of images depicted in Fig 5B'. Blue, *E. scolopes* nuclei (DAPI);
742 green, *gfp*-labeled *V. fischeri*; magenta, *hbtR* transcripts (Alexa 546).

Table 1. RNA-seq results for genes analyzed in this study[a]

Quorum-sensing genes

Locus	Gene	Product description	log2(FC)[b]	*p*-adj[c]
VF_2177	*litR*	quorum sensing transcriptional regulator LitR	-1.09	1.30E-25
VF_A0919	*luxE*	long-chain-fatty-acid ligase	-0.56	0.0002
VF_A0920	*luxB*	luciferase beta chain	-0.39	0.007
VF_A0921	*luxA*	luciferase alpha chain	-0.42	0.001
VF_A0922	*luxD*	acyl transferase	-0.36	0.027
VF_A0923	*luxC*	acyl-CoA reductase	-0.58	0.0005
VF_A0924	*luxI*	3-oxo-C6-HSL autoinducer synthesis protein	-0.67	0.0005
VF_A0925	*luxR*	LuxR family transcriptional regulator	-1.29	1.78E-27
VF_A1015	*rpoQ*	sigma-Q factor RpoQ, quorum-sensing regulated RpoS-like sigma subunit	-1.25	2.01E-14
VF_A1058	*qsrP*	LuxR family transcriptional regulator	-1.38	1.41E-05

Extracellular polysaccharide genes

Locus	Gene	Product description	log2(FC)	*p*-adj
VF_0157	*wbfB*	WbfB protein	-1.36	6.75E-21
VF_0158	VF_0158	hypothetical protein	-1.61	5.16E-23
VF_0160	*wbfD*	WbfD protein	-1.73	4.19E-14
VF_0161	VF_0161	hypothetical protein	-1.23	4.30E-28
VF_0162	*gfcE*	exopolysaccharide export protein	-1.98	8.73E-43
VF_0163	VF_0163	hypothetical protein	-1.26	2.53E-17
VF_0164	*etp*	phosphotyrosine-protein phosphatase	-2.08	1.33E-37
VF_0165	*wzc*	protein-tyrosine kinase, chain length regulator in capsular polysaccharide biosynthesis	-1.81	2.47E-38
VF_0166	*rffG*	dTDP-glucose 4,6-dehydratase	-1.98	1.01E-45
VF_0167	*rffH*	glucose-1-phosphate thymidylyltransferase	-1.65	1.01E-37
VF_0168	*rfbC*	dTDP-4-deoxyrhamnose-3,5-epimerase	-1.80	2.75E-38
VF_0169	*rmlB*	dTDP-glucose-4,6-dehydratase	-1.64	3.03E-31
VF_0170	*rfbX*	polisoprenol-linked O-antigen transporter	-1.72	3.03E-24

VF_0171	VF_0171	hypothetical protein	-1.14	1.68E-09
VF_0172	VF_0172	O-acetyltransferase	-1.64	3.26E-53
VF_0173	VF_0173	hypothetical protein	-1.94	1.66E-33
VF_0174	VF_0174	beta-D-GlcNAc beta-1,3-galactosyltransferase	-1.72	2.02E-36
VF_0175	VF_0175	glycosyltransferase	-1.50	1.16E-42
VF_0176	VF_0176	3-deoxy-8-phosphooctulonate synthase	-1.34	5.18E-30
VF_0177	VF_0177	3-deoxy-manno-octulosonate-8-phosphatase	-1.56	1.57E-56
VF_0178	VF_0178	3-deoxy-manno-octulosonate cytidylyltransferase	-1.60	1.91E-60
VF_0179	*kpsF*	arabinose-5-phosphate isomerase	-1.80	3.50E-39
VF_0180	*rfe*	UDP-GlcNAc:undecaprenylphosphate GlcNAc-1-phosphate transferase	-1.78	2.39E-71

Chemotaxis and motility genes

Locus	**Gene**	**Product description**	**log2(FC)**	***p*-adj**
VF_1133	VF_1133	methyl-accepting chemotaxis protein	1.55	4.08E-41
VF_1864	*flaC*	flagellin	1.03	1.80E-16
VF_2042	VF_2042	methyl-accepting chemotaxis protein	2.78	2.11E-87
VF_2079	*flaF*	flagellin	0.93	6.75E-16
VF_A0246	VF_A0246	methyl-accepting chemotaxis protein	1.04	8.31E-12
VF_A0389	VF_A0389	methyl-accepting chemotaxis protein	1.20	1.34E-09

[a] An abbreviated subset of data in Table S1
[b] Log 2 fold change (Δ*hbtRC*+*hbtRC* / Δ*hbtRC*)
[c] *p*-adj, Benjamini-Hochberg adjustment of Wald test *p*-value

Table 2. RT-qPCR results[a]

	Wild-type *V. fischeri*		Δ*litR*			
Gene	**ΔCt[b] (gene-*polA*)**	**SD**	**ΔCt (gene-*polA*)**	**SD**	***p*-value[c]**	**Fold change**
VF1133	3.01	0.03	1.12	0.07	0.001	3.70
VF2042	4.64	0.15	-1.73	0.52	0.002	86.13
VFA0246	3.87	0.06	-1.47	0.12	0.000	40.32
VFA0389	0.52	0.15	-0.81	0.18	0.002	2.52
cheW	-1.55	0.05	-2.53	0.24	0.019	1.99
motA1	0.95	0.23	-0.16	0.30	0.015	2.17
flaC	-1.58	0.22	-4.17	0.51	0.015	6.27
flaF	1.31	0.14	-1.44	0.75	0.024	7.41
rpoN	-0.01	0.14	0.14	0.11	0.233	0.90
flrA	-0.74	0.04	-0.48	0.12	0.071	0.84
flrB	0.85	0.13	1.38	0.63	0.293	0.74
fliA	-1.37	0.11	-1.81	0.27	0.119	1.38
flgM	-0.53	0.14	-1.35	0.31	0.053	1.80
wbfB	1.56	0.12	3.72	0.24	0.005	0.23
etp	0.38	0.09	3.42	0.08	< 0.0001	0.12
wzc	0.35	0.20	3.46	0.17	0.000	0.12

	Δ*hbtRC* + pVSV105		Δ*hbtRC* + pVSV105::*hbtRC*			
Gene	**ΔCt (gene-*polA*)**	**SD**	**ΔCt (gene-*polA*)**	**SD**	***p*-value**	**Fold change**
VF_2042	4.53	0.37	2.10	0.06	0.008	5.39
etp	-1.23	0.08	-0.26	0.08	0.0007	0.51

	Low Cell Density				High Cell Density			
Strain	**ΔCt (*hbtRC-polA*)**	**SD**	***p*-value**	**Fold change**	**ΔCt (*hbtRC-polA*)**	**SD**	***p*-value[d]**	**Fold change[d]**
Wild-type *V. fischeri*	8.08	0.12	—	—	13.07	0.35	0.002	0.03
Δ*litR*	8.19	0.58	0.775	0.97	13.02	0.69	0.007	0.04
Δ*crp*	10.06	0.68	0.038	0.27	12.29	0.12	< 0.0001	0.05

	Low Cell Density				High Cell Density			
Condition	**ΔCt (*hbtRC-polA*)**	**SD**	***p*-value**	**Fold change**	**ΔCt (*hbtRC-polA*)**	**SD**	***p*-value[e]**	**Fold change[e]**
SWT Alone	6.00	0.49	—	—	10.04	0.53	0.002	0.06
+ C8-HSL	5.72	0.13	0.473	1.25	10.60	0.87	0.001	0.06
+ 3-oxo-C6-HSL	5.71	0.39	0.432	1.22	10.16	0.26	0.004	0.05

[a] All cultures grown in SWT
[b] ΔCt, avg of three biological replicates
[c] *p*-value, Welch's t-test of ΔCt values
[d] *p*-values and fold changes compare to wild type at low density; $p > 0.05$ for Δ*litR* and Δ*crp* at high density vs. wild type at high density
[e] *p*-values and fold changes compare to wild type at low density; $p > 0.05$ for + C8-HSL and + 3-oxo-C6 at high density vs. SWT alone at high density

Table 3. Soft-agar migration zone sizes

	GlcNAc			$(GlcNAc)_2$			Neu5Ac		
Strain	**Zone size (mm)[a]**	**SD**	***p*-value[b]**	**Zone size (mm)**	**SD**	***p*-value**	**Zone size (mm)**	**SD**	***p*-value**
Wild-type *V. fischeri*	25.7	0.6	—	21.7	0.6	—	24	1	—
ΔVF_1133	18.0	0.0	< 0.0001	14.0	0.0	< 0.0001	18	1	0.002
ΔVF_2042	26.3	0.6	0.230	21.3	0.6	0.519	25	1.7	0.450
ΔVF_A0246	19.7	0.6	0.0002	16.3	0.6	0.0003	19.7	0.6	0.007
ΔVF_A0389	26.0	1.0	0.651	22.0	1.7	0.782	24	0	0.651
ΔVF_1133 ΔVF_A0246	ND[c]	ND	ND	ND	ND	ND	17.7	0.6	0.003
ΔΔΔΔ	19.3	2.1	0.037	15.3	1.2	0.014	23.7	3.2	0.880

	Glucose			No chemoattractant		
Strain	**Zone size (mm)**	**SD**	***p*-value**	**Zone size (mm)**	**SD**	***p*-value**
Wild-type *V. fischeri*	18.2	0.8	—	17.0	0.0	—
ΔΔΔΔ	19.2	2.9	0.455	16.7	0.6	0.230

	GlcNAc			No chemoattractant		
Strain	**Zone size (mm)**	**SD**	***p*-value[d]**	**Zone size (mm)**	**SD**	***p*-value[d]**
Wild-type *V. fischeri* + empty vector	10.3	1.2	—	6.0	1.0	—
Wild-type *V. fischeri* + *hbtRC*	13.7	1.2	0.024	9.0	1.0	0.021
Wild-type *V. fischeri* + *litR*	5.3	0.6	0.022	5.3	0.6	0.391
Δ*litR* + empty vector	18.7	0.6	0.008	17.7	1.5	0.002
Δ*litR* + *hbtRC*	20.7	0.6	0.011	18.3	1.2	0.002
Δ*litR* + *litR*	6.0	1.0	0.391	7.7	0.6	0.008
Δ*rpoQ* + empty vector	10.7	0.6	0.699	5.0	0.0	0.139
Δ*rpoQ* + *hbtRC*	15.3	1.2	0.152	9.7	1.5	0.572
Δ*rpoQ* + *litR*	4.7	0.6	0.230	5.3	0.6	1.000

[a] Average of ≥ three biological replicates.
[b] *p*-value, Welch's t-test as compared to wild-type zones in that chemoattractant.
[c] ND, not done.
[d] *p*-value for wild-type strains, as compared to wild type carrying empty vector; for Δ*litR* and Δ*rpoQ* strains, as compared to wild type carrying the respective vector.

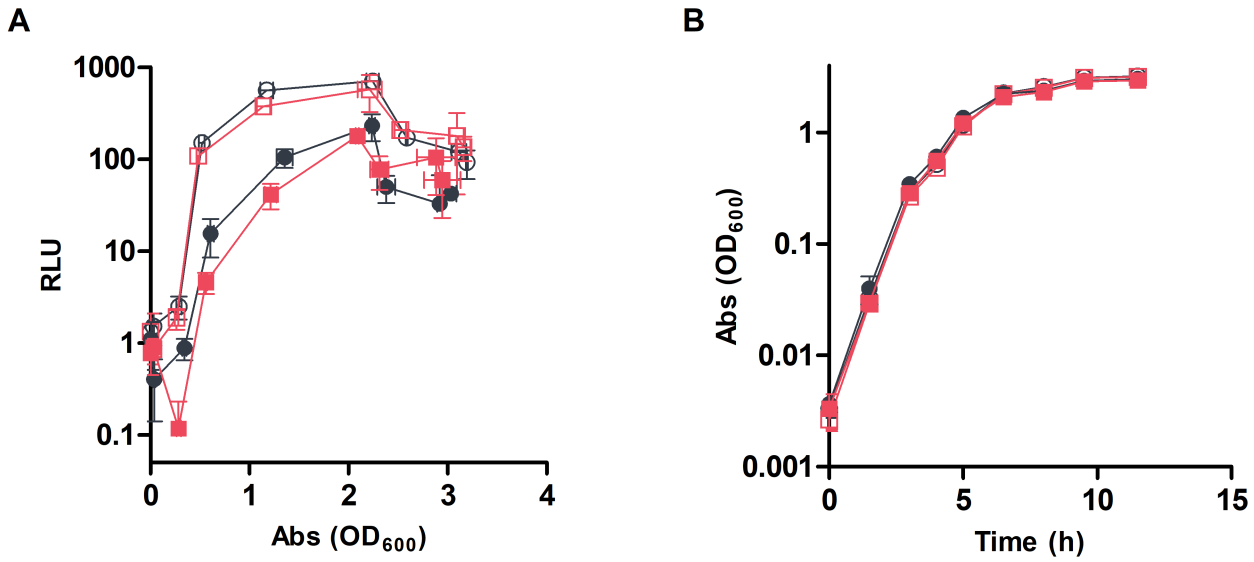
A
1000
100
10
1
0.1
RLU
0
1
2
3
4
Abs (OD600)
B
1
0.1
0.01
0.001
Abs (OD600)
0
5
10
15
Time (h)

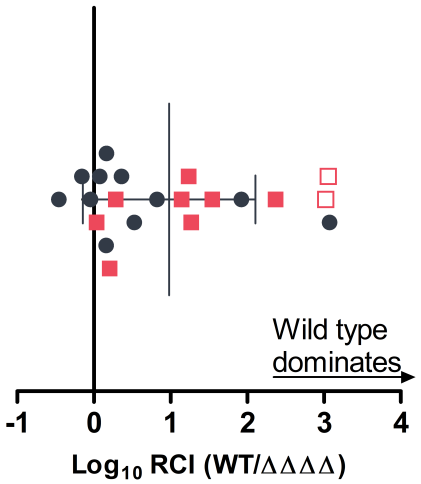
Wild type
dominates
-1
0
1
2
3
4
Log10 RCI (WT/ΔΔΔΔ)

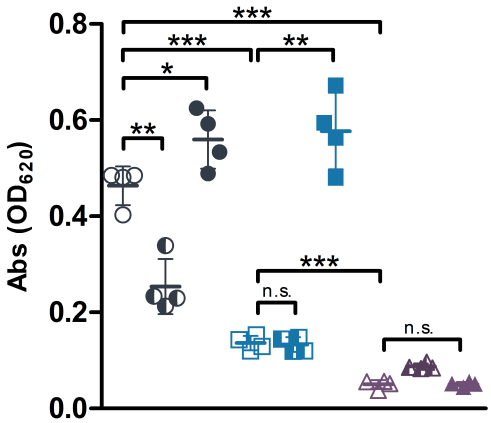
0.8
0.6
0.4
0.2
0.0
Abs (OD620)
***
***
**
*
**
***
n.s.
n.s.

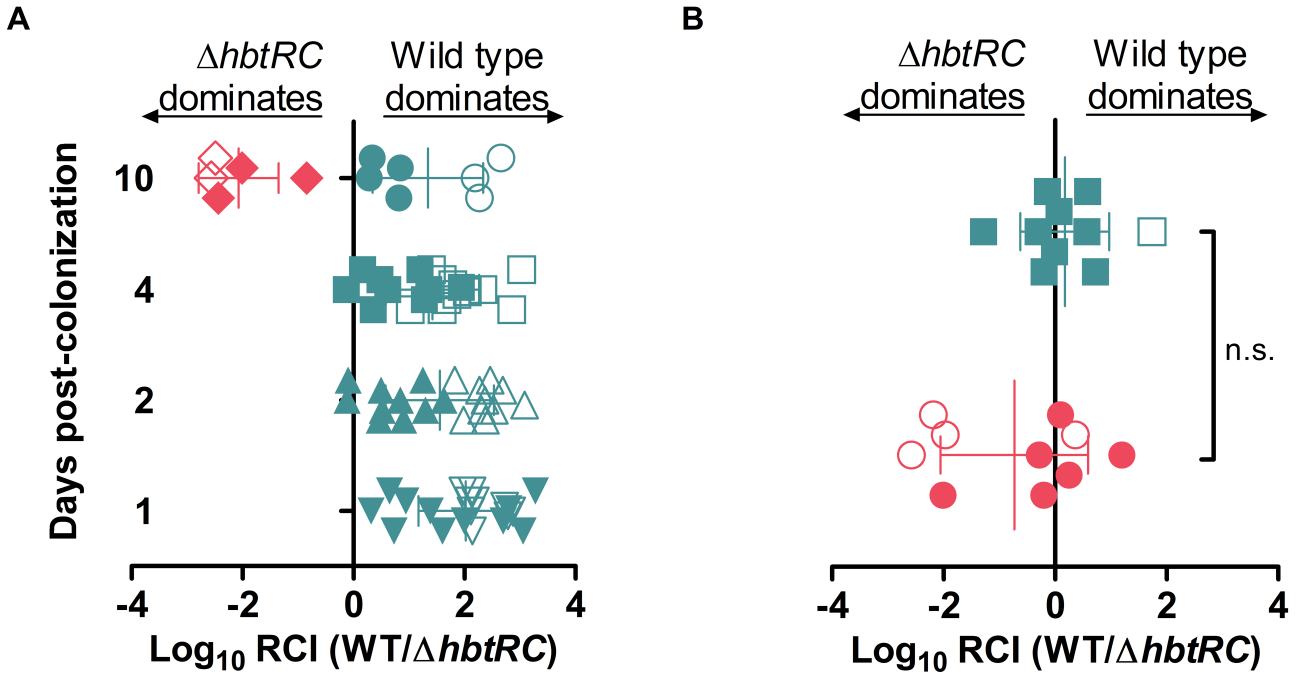
A
ΔhbtRC dominates
Wild type dominates
Days post-colonization
10
4
2
1
-4
-2
0
2
4
Log10 RCI (WT/ΔhbtRC)
B
ΔhbtRC dominates
Wild type dominates
n.s.
-4
-2
0
2
4
Log10 RCI (WT/ΔhbtRC)

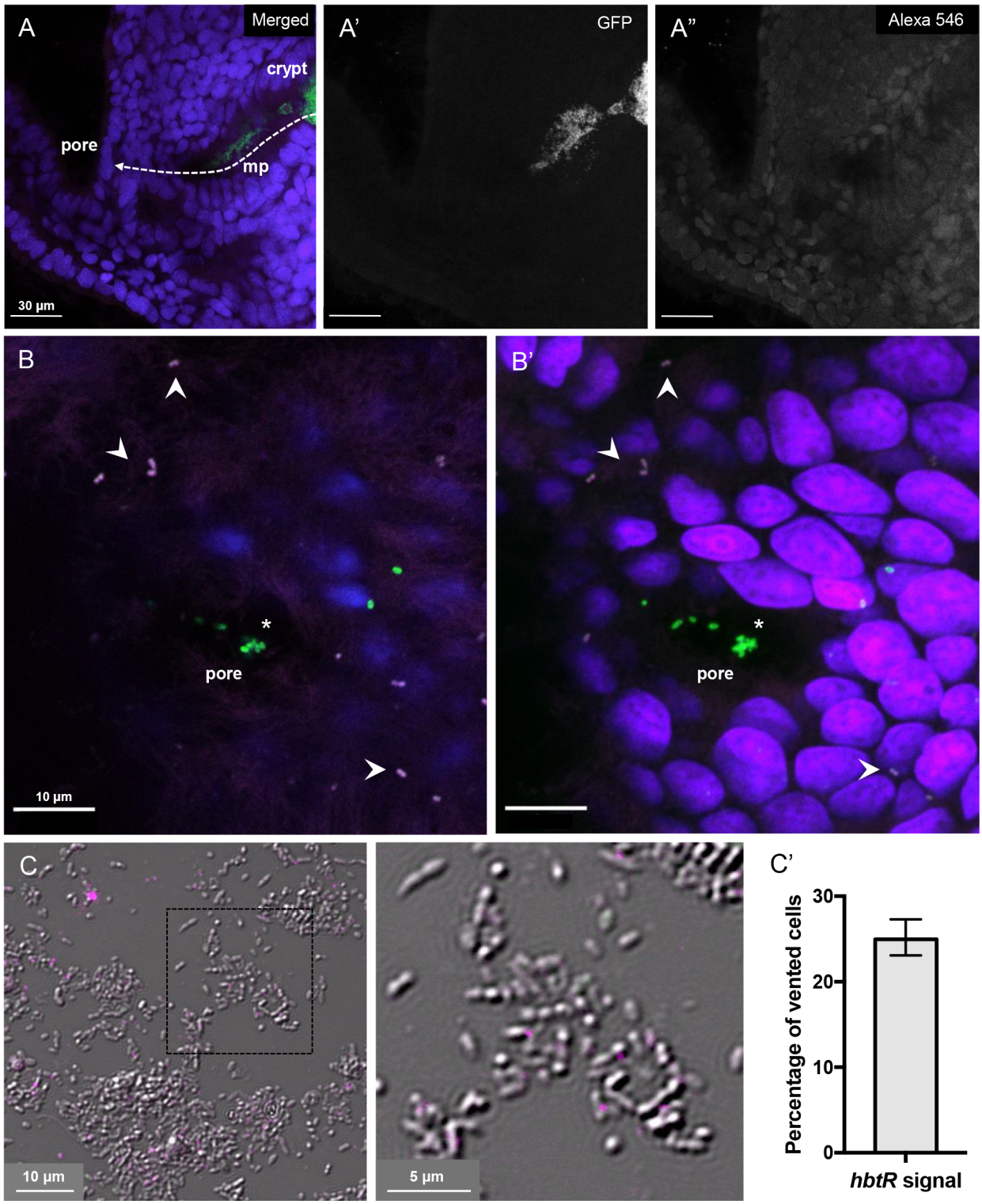
A
Merged
crypt
pore
mp
30 µm
A'
GFP
A"
Alexa 546
B
pore
10 µm
B'
pore
C
10 µm
5 µm
C'
Percentage of vented cells
30
20
10
0
hbtR signal

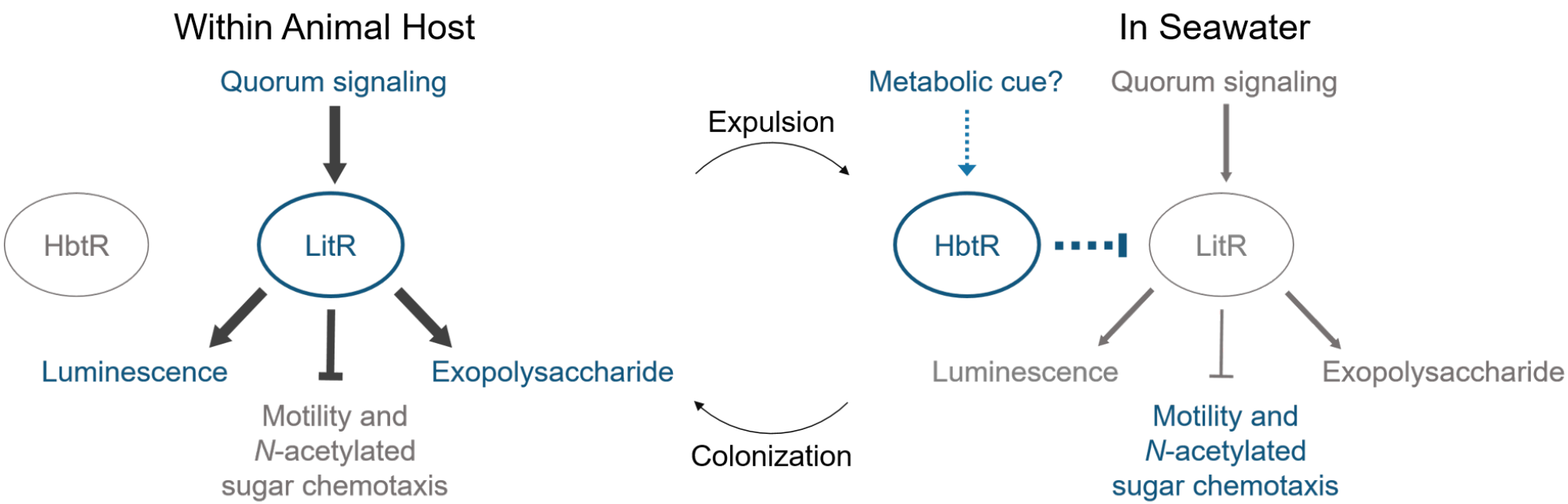
Within Animal Host
Quorum signaling
HbtR
LitR
Luminescence
Motility and
N-acetylated
sugar chemotaxis
Exopolysaccharide
Expulsion
Colonization
In Seawater
Metabolic cue?
Quorum signaling
HbtR
LitR
Luminescence
Motility and
N-acetylated
sugar chemotaxis
Exopolysaccharide